

standing of Kondo systems it is not so much which theoretical description is most appropriate, but rather that both models, which were developed to interpret spin-compensated Kondo systems, appear to be applicable to this particular dilute alloy, Pt-Co; a giant moment system.¹¹ Hence it appears, insofar as the

resistivity and magnetic properties are concerned, that this system behaves phenomenologically as if the local moment were a single entity scattered from and spin compensated in a manner not unlike the nongiant moment local moment systems such as *Rh-Fe* or a "classical" Kondo system like *Cu-Fe*.

¹¹ The absence of any observable Co concentration dependence outside of that expected from noninteracting Co moments as seen

in the NMR results of Ref. 3 indicates that correlations, if present, are probably not significant for our results.

PHYSICAL REVIEW

VOLUME 179, NUMBER 2

10 MARCH 1969

Anisotropy of the Europium-Iron Exchange Interaction in Rare-Earth Iron Garnets*

U. ATZMONY, E. R. BAUMINGER, A. MUSTACHI, I. NOWIK, S. OFER, AND M. TASSA
Department of Physics, The Hebrew University, Jerusalem, Israel
 (Received 28 June 1968)

Mössbauer studies of the 21.6-keV transition of Eu^{151} and the 14.4-keV transition of Fe^{57} in europium iron garnet, samarium iron garnet, and mixed samarium-europium iron garnets were performed at various temperatures. The recoilless absorption spectra of the 21.6-keV and 14.4-keV γ rays in SmIG and in $\{\text{Sm}_x\text{Eu}_{1-x}\}\text{IG}$ at 4.2°K differ substantially from the spectra in EuIG and other rare-earth iron garnets. The main conclusions drawn from the experimental results are the following. (1) The Eu-Fe exchange interaction in the garnets is anisotropic. The principal values of the anisotropic exchange field acting on the Eu^{3+} ions (produced mainly by the Fe^{3+} ions in the tetrahedral sites) are $\beta H_z/hc = 12.7 \text{ cm}^{-1}$, $\beta H_y/hc = 11.9 \text{ cm}^{-1}$, and $\beta H_x/hc = 20.3 \text{ cm}^{-1}$. (2) The anisotropic properties of the Eu^{3+} ions in the garnets are mainly produced by the anisotropy in the Eu-Fe exchange interaction and not by the crystalline-field interactions. (3) The direction of the tetrahedral iron sublattice magnetization (\mathbf{n}_d) in SmIG at 4.2 and 20°K and in mixed $\{\text{Sm}_x\text{Eu}_{1-x}\}\text{IG}$'s with $x \geq 0.05$ at 4.2°K is close to the [110] direction of the cubic unit cell. The experimental results tend to indicate that the direction of \mathbf{n}_d in SmIG and in mixed Eu-Sm garnet at 4.2°K makes a small angle ($\sim 5^\circ$) with the [110] direction of the unit cell, and that the direction of \mathbf{n}_d at 85°K is slightly canted relative to the [111] direction.

INTRODUCTION

THE anisotropy of the exchange interactions in rare-earth iron garnets was recently studied experimentally¹⁻³ and theoretically.⁴⁻⁶ The experiments were limited mainly to the case of ytterbium iron garnet (YbIG). Since Mössbauer studies of Eu^{3+} isotopes yield detailed information concerning exchange interactions,⁷ we have carried out Mössbauer effect measurements on Eu nuclei in europium iron garnet (EuIG), samarium iron garnet (SmIG), and mixed Eu-Sm iron garnets at various temperatures, with the intention of studying the anisotropy of the Eu-Fe exchange interactions in the garnets.

Some recoilless absorption measurements of the 14.4-keV γ rays of Fe^{57} in various garnet systems were also

carried out in order to verify our conclusions concerning the direction of easy magnetization in SmIG at various temperatures.

Almost all of the recoilless absorption measurements with Eu nuclei were carried out using the 21.6-keV γ ray of Eu^{151} . This γ ray was chosen because well-resolved lines are obtained in its recoilless absorption spectra in magnetically ordered Eu compounds.

For the studies carried out on Eu^{3+} ions in SmIG, a Sm^{151}IG source and an Eu_2O_3 absorber were used and the splittings observed corresponded to the hyperfine interactions in the source. For the studies of Eu^{3+} ions in EuIG and in mixed garnets, a source of $\text{Sm}_2^{151}\text{O}_3$ and garnet absorbers were used. The splittings observed in these cases were produced by the hyperfine interactions in the absorbers.

The crystal structure of the garnets is well known.^{8,9} The cubic unit cell contains eight formula units of $\text{R}_3\text{Fe}_5\text{O}_{12}$. Assuming a general direction for a magnetic or an exchange field, there are six magnetically inequivalent sites for the rare-earth ions in each unit cell of the

* Supported in part by the Israel Academy of Sciences and Humanities.

¹ K. A. Wickersheim, *Phys. Rev.* **122**, 1376 (1961).

² K. A. Wickersheim and R. L. White, *Phys. Rev. Letters* **4**, 123 (1960).

³ A. J. Sievers and M. Tinkham, *Phys. Rev.* **129**, 1995 (1963).

⁴ W. P. Wolf, *Proc. Phys. Soc. (London)* **74**, 665 (1959).

⁵ P. M. Levy, *Phys. Rev.* **135**, A155 (1964).

⁶ P. M. Levy, *Phys. Rev.* **147**, 311 (1966).

⁷ I. Nowik and S. Ofer, *Phys. Rev.* **153**, 409 (1967).

⁸ G. Menzer, *Z. Krist.* **69**, 300 (1929).

⁹ S. Geller and M. A. Gilleo, *J. Phys. Chem. Solids* **3**, 30 (1957).

iron garnets (the inequivalent sites differ in the direction of \mathbf{H}_{ex} relative to the local principal axes of the crystal-line electric fields). In most of the rare-earth iron garnets, the magnetization is in the [111] direction of the unit cell, and two inequivalent sites with equal multiplicities exist. In SmIG at low temperatures the easy magnetization is probably along the [110] direction,¹⁰⁻¹² resulting in three inequivalent sites with relative multiplicities 4:1:1.

The hyperfine splittings of the 21.6-keV transition of Eu¹⁵¹ and the 103-keV transition of Eu¹⁵³ in EuIG were measured in previous works.¹³⁻¹⁵ The spectra obtained indicated that the difference between the values of H_{eff} corresponding to the two magnetically inequivalent sites in EuIG is small. Atzmony *et al.*¹⁶ have estimated the exchange magnetic field at Eu ions inside various rare-earth iron garnets (RIGs) from measurements of the splittings of the 103-keV Mössbauer line of Eu¹⁵³ with sources of the composition $(R_{0.975}\text{Sm}^{153}_{0.025})_3\text{Fe}_5\text{O}_{12}$ and an Eu₂O₃ absorber. They found that the spectra obtained for Eu³⁺ in all RIGs except SmIG were very similar in shape to that obtained in EuIG. For Eu³⁺ in SmIG they found a different spectrum, which was explained as due to the different direction of the easy magnetization in SmIG. In the present work, the spectra obtained for Eu³⁺ in SmIG and in mixed Eu-Sm iron garnets at 4.2°K, using the 21.6-keV γ ray of Eu¹⁵¹, were found to be very different from those obtained with an EuIG absorber. Their general shape is consistent with the interpretation that they are composed of three sub-spectra with relative intensities of 4:1:1, as expected when the magnetization is in the [110] direction. The analysis of these spectra proves that the Eu-Fe exchange interaction is very anisotropic. The principal values of the exchange field acting on an Eu³⁺ ion in the garnets at 4.2°K are

$$\beta H_x/hc = 12.7 \text{ cm}^{-1}, \quad \beta H_y/hc = 11.9 \text{ cm}^{-1},$$

and

$$\beta H_z/hc = 20.3 \text{ cm}^{-1}.$$

THEORY

A. Anisotropic Exchange Hamiltonian

Wolf⁴ has suggested that the rare-earth-iron (RE-Fe) exchange interaction should be anisotropic from considerations of the anisotropic or "spiked" nature of the $4f$ orbital wave function of the rare-earth ion.

The Hamiltonian of the exchange interaction between an Fe³⁺ ion and a rare-earth ion can be written in the

following form⁵:

$$\mathcal{H} = 2J(L, L_z)\mathbf{S}(\text{RE}) \cdot \mathbf{S}(\text{Fe}). \quad (1)$$

The exchange integral J , which is a constant in the ordinary isotropic Heisenberg Hamiltonian, is now an operator in the rare-earth angular momenta. The operator $J(L, L_z)$ can be expanded in terms of spherical harmonic operators:

$$J(L, L_z) = J_0 \left[1 + \sum_{m,n} G_n^m Y_n^m(L, L_z) \right]. \quad (2)$$

Assuming that the exchange operator has the local point symmetry of the rare-earth ion, only a few n and m values are allowed in the expansion. For rare-earth ions ($4f$ electrons), in the orthorhombic symmetry of the garnet, only ten parameters in the expansion must be considered (J_0 and G_n^m , where $n=2, 2, 4, 4, 6, 6, 6, 6, 6, 6$).

According to previous work, the interactions between the c and a sublattices in the garnets are negligible compared to the interactions between the c and d sublattices,^{7,17-20} and thus $\mathbf{S}(\text{Fe})$ in Eq. (1) can be replaced by $\mathbf{S}_d(\text{Fe})$.

The Hamiltonian of the exchange interaction between the Fe³⁺ ions and a rare-earth ion can also be expressed in the more familiar form¹⁷

$$\mathcal{H} = 2\beta \mathbf{S}(\text{RE}) \cdot \mathbf{A} \cdot \mathbf{S}_d(\text{Fe}), \quad (3)$$

where \mathbf{A} is an exchange tensor. If we define a vector \mathbf{H}_{ex} by

$$\mathbf{H}_{\text{ex}} = \mathbf{A} \cdot \mathbf{S}_d(\text{Fe}), \quad (4)$$

then (3) obtains its usual (formal) isotropic form:

$$\mathcal{H} = 2\beta \mathbf{S}(\text{RE}) \cdot \mathbf{H}_{\text{ex}}. \quad (5)$$

In the simple molecular field approximation, $\mathbf{S}_d(\text{Fe})$ is replaced by its expectation value, which is proportional to the tetrahedral iron sublattice magnetization $M_d(T)$. Thus, one obtains

$$\mathbf{H}_{\text{ex}}(T) = S_{\text{Fe}} [M_d(T)/M_d(0)] \mathbf{A} \cdot \mathbf{n}_d. \quad (6)$$

Here $S_{\text{Fe}} = \frac{5}{2}$, and \mathbf{n}_d is a unit vector in the direction of the tetrahedral (d) sublattice iron magnetization. \mathbf{H}_{ex} is not parallel to \mathbf{n}_d and its magnitude depends on the direction of \mathbf{n}_d .

It is usually assumed that the exchange tensor \mathbf{A} is diagonal in the principal axes of the local crystalline field at the rare-earth-ion site. Hence the expressions for

¹⁰ C. Nowlin and R. V. Jones, J. Appl. Phys. **34**, 1262 (1963);

C. Nowlin, Ph.D. thesis, Harvard University, 1963 (unpublished).

¹¹ R. F. Pearson, J. Appl. Phys. **33**, 1236 (1962).

¹² J. A. White, Proc. Phys. Soc. (London) **90**, 1095 (1967).

¹³ I. Nowik and S. Ofer, Phys. Rev. **132**, 241 (1963).

¹⁴ P. Kienle, Rev. Mod. Phys. **36**, 372 (1964).

¹⁵ U. Atzmony, A. Mualem, and S. Ofer, Phys. Rev. **136**, B1237 (1964).

¹⁶ U. Atzmony, E. R. Bauminger, B. Einhorn, J. Hess, A. Mustachi, and S. Ofer, J. Appl. Phys. **39**, 1250 (1968).

¹⁷ T. Hutchings, C. G. Windsor, and W. P. Wolf, Phys. Rev. **148**, 444 (1966).

¹⁸ S. Geller, H. J. Williams, R. C. Sherwood, and G. P. Espinosa, J. Appl. Phys. **36**, 88 (1965).

¹⁹ R. C. LeCraw, J. P. Remeika, and H. Matthews, Phys. Letters **12**, 9 (1964); J. Appl. Phys. **36**, 901 (1965).

²⁰ S. M. Myers, J. P. Remeika, and H. Meyer, Phys. Rev. **170**, 520 (1968).

\mathbf{H}_{ex} and $|\mathbf{H}_{\text{ex}}|$ at 0°K are

$$\mathbf{H}_{\text{ex}}(0^\circ\text{K}) = \frac{5}{2}\mathbf{A} \cdot \mathbf{n}_d, \quad (7a)$$

$$|\mathbf{H}_{\text{ex}}(0^\circ\text{K})| = \frac{5}{2}(A_x^2 n_x^2 + A_y^2 n_y^2 + A_z^2 n_z^2)^{1/2} \\ = (H_x^2 n_x^2 + H_y^2 n_y^2 + H_z^2 n_z^2)^{1/2}. \quad (7b)$$

$|\mathbf{H}_{\text{ex}}(0^\circ\text{K})|$ can also be expressed in the form

$$|\mathbf{H}_{\text{ex}}(0^\circ\text{K})| = \bar{H}_{\text{ex}}(\mu_x^2 n_x^2 + \mu_y^2 n_y^2 + \mu_z^2 n_z^2)^{1/2}, \quad (7c)$$

where

$$\bar{H}_{\text{ex}} = \frac{1}{3}(H_x + H_y + H_z), \quad \mu_x = 3A_x/(A_x + A_y + A_z), \\ \mu_y = 3A_y/(A_x + A_y + A_z), \quad \text{and} \quad \mu_z = 3A_z/(A_x + A_y + A_z).$$

B. Eu^{3+} Ions in an Anisotropic Exchange Field

The ionic ground state of Eu^{3+} is 7F_0 , which is diamagnetic. The separation (Δ_1) between the first excited ionic state ($J=1$) and the ground state is only about 480°K . Therefore, the exchange interaction mixes the excited state into the ground state and produces nonvanishing magnetic moments and hyperfine fields.^{21,22}

First-order perturbation theory yields the following expressions for the magnetic moment and internal effective magnetic field at 0°K ^{21,22}:

$$\mathbf{M}_{\text{Eu}}(0^\circ\text{K}) = (16\beta^2/\Delta_1)\mathbf{H}_{\text{ex}} = (40\beta^2/\Delta_1)\mathbf{A} \cdot \mathbf{n}_d, \quad (8)$$

$$\mathbf{H}_{\text{eff}}(0^\circ\text{K}) = (-80\beta^2/3\Delta_1)\langle 1/r^3 \rangle \mathbf{H}_{\text{ex}} \\ = (-200\beta^2/3\Delta_1)\langle 1/r^3 \rangle \mathbf{A} \cdot \mathbf{n}_d = \alpha \mathbf{A} \cdot \mathbf{n}_d, \quad (9a)$$

$$|\mathbf{H}_{\text{eff}}(0^\circ\text{K})| = \bar{H}_{\text{eff}}(\mu_x^2 n_x^2 + \mu_y^2 n_y^2 + \mu_z^2 n_z^2)^{1/2}, \quad (9b)$$

where $\bar{H}_{\text{eff}} = \frac{1}{3}\alpha(A_x + A_y + A_z)$. μ_x , μ_y , and μ_z were defined in Eq. (7c).

The values of A_x , A_y , and A_z can be expressed in terms of the more fundamental exchange parameters J_0 and G_n^m . If in the expansion of $J(L, L_z)$ [Eq. (2)] terms higher than $n=2$ are neglected, then A_x , A_y , and A_z can be calculated as functions of J_0 , G_2^0 , and G_2^2 . Under those assumptions, the exchange Hamiltonian [Eq. (1)] is given by

$$\mathcal{H} = 2J_0\{1 + G_2^0[2L_z^2 - L(L+1)] \\ + G_2^2[L_+^2 + L_-^2]\}\mathbf{S}(\text{Eu}) \cdot \mathbf{S}(\text{Fe}), \quad (10)$$

and, from first-order perturbation theory, the following expressions for A_x , A_y , and A_z are obtained:

$$A_x = J_0\mu_x = J_0(1 - \frac{9}{2}G_2^0 + 9G_2^2), \\ A_y = J_0\mu_y = J_0(1 - \frac{9}{2}G_2^0 - 9G_2^2), \quad (11) \\ A_z = J_0\mu_z = J_0(1 + 9G_2^0).$$

The above expressions were calculated in first-order perturbation theory for the ground-state wave function. Crystalline-field effects were neglected. If one also takes into account the mixing effects of the crystalline-field

potential V_c ,

$$V_c = \sum_{n,m} A_n^m \langle r^n \rangle \langle ||\alpha_n|| \rangle O_n^m, \quad (12)$$

where all the symbols have their conventional meaning,²³ then third-order perturbation theory yields the following expressions for $\mathbf{M}_{\text{Eu}}(0^\circ\text{K})$ and $\mathbf{H}_{\text{eff}}(0^\circ\text{K})$:

$$\mathbf{M}(0^\circ\text{K}) = (40\beta^2/\Delta_1)\mathbf{B} \cdot \mathbf{n}_d, \quad (13)$$

where

$$B_x = J_0(1 - \frac{9}{2}G_2^0 + 9G_2^2 - A_2^0 \langle r^2 \rangle / 5\Delta_1 + A_2^2 \langle r^2 \rangle / 5\Delta_1 \\ - A_2^0 \langle r^2 \rangle / 5\Delta_2 + A_2^2 \langle r^2 \rangle / 5\Delta_2), \\ B_y = J_0(1 - \frac{9}{2}G_2^0 - 9G_2^2 - A_2^0 \langle r^2 \rangle / 5\Delta_1 - A_2^2 \langle r^2 \rangle / 5\Delta_1 \\ - A_2^0 \langle r^2 \rangle / 5\Delta_2 - A_2^2 \langle r^2 \rangle / 5\Delta_2), \\ B_z = J_0(1 + 9G_2^0 + 2A_2^0 \langle r^2 \rangle / 5\Delta_1 + 2A_2^2 \langle r^2 \rangle / 5\Delta_2),$$

and

$$\mathbf{H}_{\text{eff}} = (-200\beta^2/3\Delta_1)\langle 1/r^3 \rangle \mathbf{C} \cdot \mathbf{n}_d, \quad (14)$$

where

$$C_x = J_0(1 - \frac{9}{2}G_2^0 + 9G_2^2 - A_2^0 \langle r^2 \rangle / 5\Delta_1 + A_2^2 \langle r^2 \rangle / 5\Delta_1 \\ - 51A_2^0 \langle r^2 \rangle / 250\Delta_2 + 51A_2^2 \langle r^2 \rangle / 250\Delta_2), \\ C_y = J_0(1 - \frac{9}{2}G_2^0 - 9G_2^2 - A_2^0 \langle r^2 \rangle / 5\Delta_1 - A_2^2 \langle r^2 \rangle / 5\Delta_1 \\ - 51A_2^0 \langle r^2 \rangle / 250\Delta_2 - 51A_2^2 \langle r^2 \rangle / 250\Delta_2), \\ C_z = J_0(1 + 9G_2^0 + 2A_2^0 \langle r^2 \rangle / 5\Delta_1 + 51A_2^2 \langle r^2 \rangle / 125\Delta_2).$$

The crystal-field parameters for Eu^{3+} in EuIG as given by Koningstein²⁴ are $A_2^0 \langle r^2 \rangle = 105 \text{ cm}^{-1}$ and $A_2^2 \langle r^2 \rangle = \pm 95 \text{ cm}^{-1}$. Using these parameters and Eq. (14), the anisotropy in \mathbf{H}_{eff} produced by the crystalline-field interaction is found to be about 10%. Since the experiments carried out in the present work show that the anisotropy is much larger, the conclusion is that the anisotropic nature of the RE-Fe exchange interaction and not the crystalline-field interaction is the main reason for the anisotropy of \mathbf{H}_{ex} and \mathbf{H}_{eff} .

EXPERIMENTAL DETAILS

Two Sm^{151} -fission product sources were used for the recoilless absorption measurements of the 21.6-keV γ ray of Eu^{151} . One source was in the form of Sm_2O_3 and the other in the form of SmIG. The source used for the recoilless absorption measurements of the 103-keV γ ray of Eu^{153} was Sm^{153} in the form of SmIG. This source was produced by neutron irradiation of 15 mg of SmIG for 10 h in a flux of 10^{13} neutrons/sec. The γ radiations were detected in both cases by a 4-mm-thick NaI(Tl) scintillation counter with a Be window.

The following absorbers were used for the 21.6-keV γ ray emitted by the $\text{Sm}_2^{151}\text{O}_3$ sources: EuIG, $\{\text{Eu}_{0.5}\text{Sm}_{0.5}\}\text{IG}$, $\{\text{Eu}_{0.75}\text{Sm}_{0.25}\}\text{IG}$, and $\{\text{Eu}_{0.95}\text{Sm}_{0.05}\}\text{IG}$. The thickness of all these absorbers was $\sim 100 \text{ mg/cm}^2$. An absorber of 40 mg/cm^2 Eu_2O_3 enriched to

²¹ W. P. Wolf and J. M. Van Vleck, Phys. Rev. **118**, 1490 (1960).

²² G. Gilat and I. Nowik, Phys. Rev. **130**, 1361 (1963).

²³ M. T. Hutchings, Solid State Phys. **16**, 227 (1966).

²⁴ J. A. Koningstein, J. Chem. Phys. **42**, 3193 (1965).

80% in Eu^{151} was used together with the Sm^{151}IG source.

All the above measurements were carried out with both source and absorber at the same temperature, using a cryostat filled with liquid helium, liquid hydrogen, or liquid air. Both source and absorbers were immersed in the respective liquids.

Recoilless absorption measurements of the 14.4-keV γ ray of Fe^{57} in EuIG and SmIG at 4, 20, 85, and 300°K were also performed. The source consisted of 10 mCi Co^{57} in Pt at room temperature, and the various absorbers had a thickness of 20 mg/cm². In addition, absorption measurements of the 14.4-keV γ ray at room temperature, or slightly above it, were also carried out with absorbers of substituted garnets: $\text{Eu}_3\text{Sc}_{1.5}\text{Fe}_{3.5}\text{O}_{12}$, $\text{Eu}_3\text{Sc}_1\text{Fe}_4\text{O}_{12}$, and $\text{Eu}_3\text{Ga}_{1.6}\text{Fe}_{3.4}\text{O}_{12}$. As a detector for the 14.4-keV γ radiation, a 0.1-mm-thick NaI(Tl) scintillation counter with a Be window was used. All the garnet samples used as absorbers were analyzed by x rays. Their powder photographs or diffractometer patterns were carefully analyzed in order to be sure that single phases were obtained. The lattice constants were measured and found to be consistent with the systematic behavior of the lattice constants of the respective garnet systems.^{18,25,26} Some of the values of the lattice con-

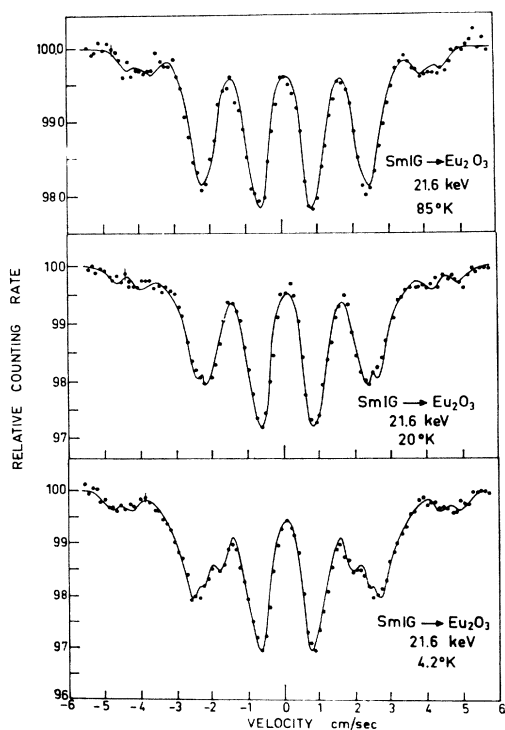


FIG. 1. Recoilless absorption spectra of the 21.6-keV γ ray, emitted from a Sm^{151}IG source, in a Eu_2O_3 absorber. The solid lines are the theoretical spectra, computed with the parameters given in the text and in Table IV.

²⁶ G. P. Espinosa, J. Chem. Phys. 37, 2344 (1962).

²⁵ S. Geller, J. A. Cape, G. P. Espinosa, and D. H. Leslie, Phys. Rev. 148, 522 (1966).

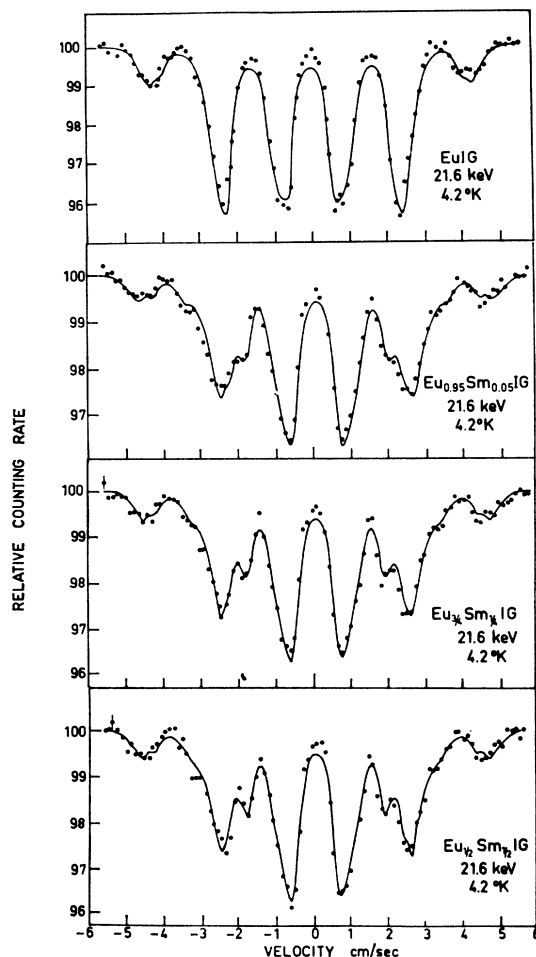


FIG. 2. Recoilless absorption spectra of the 21.6-keV γ ray, emitted from a $\text{Sm}^{151}\text{O}_3$ source, in EuIG and mixed $\{\text{Eu}_x\text{Sm}_{1-x}\}\text{IG}$ absorbers. The solid lines are the theoretical spectra computed with the parameters given in the text and in Table IV.

stants determined in the present work, which are not found in the literature, are given in Table I. The preparation of the samples required, in many cases, several regrindings and refirings.

The counting rate as a function of relative velocity between source and absorber was measured using an apparatus similar to the one described by Cohen *et al.*²⁷ The recoilless absorption spectra were recorded automatically on a multichannel pulse-height analyzer work-

TABLE I. Sizes of unit cell of some garnets determined in the present work.

Compound	Cubic unit cell dimension (Å)
$\{\text{Eu}_{0.5}\text{Sm}_{0.5}\}\text{IG}$	12.512 ± 0.005
$\text{Eu}_3\text{Sc}_1\text{Fe}_4\text{O}_{12}$	12.572 ± 0.005
$\text{Eu}_3\text{Sc}_{1.5}\text{Fe}_{3.5}\text{O}_{12}$	12.606 ± 0.005

²⁷ R. L. Cohen, P. G. McMullin, and G. K. Wertheim, Rev. Sci. Instr. 34, 671 (1963).

TABLE II. The components of \mathbf{n}_d along the local axes of the rare-earth sites in the garnets. a , b , and c are the components of \mathbf{n}_d along the axes of the cubic cell.

Site No.	n_x	n_y	n_z
1	$(b+c)\frac{1}{2}\sqrt{2}$	$(b-c)\frac{1}{2}\sqrt{2}$	a
2	$(b-c)\frac{1}{2}\sqrt{2}$	$(b+c)\frac{1}{2}\sqrt{2}$	a
3	$(c+a)\frac{1}{2}\sqrt{2}$	$(c-a)\frac{1}{2}\sqrt{2}$	b
4	$(c-a)\frac{1}{2}\sqrt{2}$	$(c+a)\frac{1}{2}\sqrt{2}$	b
5	$(a+b)\frac{1}{2}\sqrt{2}$	$(a-b)\frac{1}{2}\sqrt{2}$	c
6	$(a-b)\frac{1}{2}\sqrt{2}$	$(a+b)\frac{1}{2}\sqrt{2}$	c

ing in the multiscaler mode. The absorption spectra were folded automatically in the multichannel analyzer.²⁸

EXPERIMENTAL RESULTS

A. Recoilless Absorption of the 21.6-keV γ Ray of Eu^{151}

The absorption spectra in a Eu_2O_3 absorber of the 21.6-keV γ ray of Eu^{151} , emitted from a Sm^{151}IG source, with both source and absorber at 4.2, 20, and 85°K, are shown in Fig. 1. The recoilless absorption spectra of the 21.6-keV γ ray emitted from a $\text{Sm}_2^{151}\text{O}_3$ source and using a EuIG and mixed {Eu-Sm}IG absorbers at 4.2°K are shown in Fig. 2. In the spectra shown in Fig. 1, the splittings are due to internal hyperfine interactions in the source, whereas in the spectra shown in Fig. 2 the splittings are produced by the hyperfine interactions in the absorber.

As has been shown in the Introduction, the effective magnetic field acting on the Eu nuclei in garnets is equal to $\alpha\mathbf{A}\cdot\mathbf{n}_d$, where \mathbf{n}_d represents the unit vector in the direction of the easy magnetization of the d sites. For an arbitrary direction of \mathbf{n}_d , one can expect six different fields acting on the Eu nuclei in the six inequivalent sites. The components of \mathbf{n}_d with respect to the local axes at each of the six sites are given in Table II. The components are expressed in terms of a , b , and c , which are the components of \mathbf{n}_d along the cubic axes of the

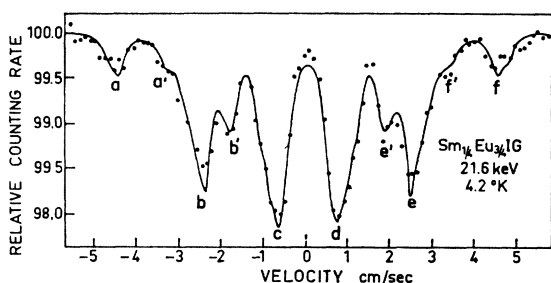


FIG. 3. Recoilless absorption spectrum of the 21.6-keV γ ray, emitted from a $\text{Sm}^{151}\text{O}_3$ source, in a $\{\text{Eu}_{0.75}\text{Sm}_{0.25}\}$ IG absorber. The solid line is the theoretical spectrum computed with the parameters given in Table III.

²⁸ E. Nadav and M. Palmai, Nucl. Instr. Methods **56**, 165 (1967).

crystallographic unit cell. Using Table II and Eq. (9b), we have calculated expressions for $|\mathbf{H}_{\text{eff}}|$ at the six sites, as a function of a , b , c , \bar{H}_{eff} , μ_x , μ_y , and μ_z .

As pointed out in the Introduction, the direction of magnetization in most RIGs is known to be in the $[111]$ direction, whereas there are some indications that the magnetization of SmIG at low temperatures is in the $[110]$ direction.¹⁰⁻¹² It is seen clearly from Figs. 1 and 2 that the recoilless absorption spectrum obtained with EuIG at 4.2°K differs substantially from the spectra obtained with Eu^{3+} in SmIG and in mixed {Eu-Sm}IG absorbers at 4.2°K. All the spectra of the mixed garnets are very similar. Even a garnet containing 5% Sm and 95% Eu gives a spectrum similar to the one with a SmIG source and a Eu_2O_3 absorber. The spectrum obtained with the EuIG absorber can be explained as a superposition of two spectra of equal intensity, one corresponding to an internal field of 611 kOe and the other to an internal field of 564 kOe. The general shape of all the other spectra at 4.2°K can be explained assuming that they are composed of three subspectra with relative intensities of 4:1:1, as expected when \mathbf{n}_d is in the $[110]$ direction. Theoretical fits to the experimental spectra were calculated under these assumptions and are shown for EuIG in Fig. 2 (the solid line) and for $\{\text{Eu}_{0.75}\text{Sm}_{0.25}\}$ IG in Fig. 3. Peaks a , b , e , and f , in the absorption spectrum in Fig. 3, are produced by the highest point symmetry sites, while peaks a' , b' , e' , and f' are produced by the Eu nuclei in the two other inequivalent sites. All sites contribute to peaks c and d . Further assumptions made in the construction of the theoretical spectra were the following: Each individual absorption line has a Lorentzian shape with a full width at half-height of 3.45 mm/sec. (This width was deduced from the absorption spectrum obtained with a Sm_2O_3 source and a Eu_2O_3 absorber. The reconstructed spectrum is quite insensitive to small changes in this line-width.) The ratio of the g factors of the 21.6-keV excited state and the ground state in $\text{Eu}^{151}(g_e/g_0)$ is 0.532,^{7,14} and the magnetic moment of the ground state is $3.464\mu_N$.²⁹ Because of the symmetrical shape of all the experimental spectra, quadrupole interactions were assumed to be negligible. The values of $|\mathbf{H}_{\text{eff}}|$ in the three Eu^{3+} sites which were used in the reconstruction of Fig. 3 are given in Table III. The table also includes the parameters derived for a Eu^{3+} ion in SmIG under the above assumptions. The fits obtained are seen to be

TABLE III. Effective magnetic fields and anisotropy parameters giving the best fit to experimental results at 4.2°K, assuming \mathbf{n}_d to be strictly in the $[110]$ direction. s.p. = relative site population.

Compound	H_{eff} (kOe)			\bar{H}_{eff} (kOe)	μ_x	μ_y	μ_z
	s.p. = 4	s.p. = 1	s.p. = 1				
Eu^{3+} in SmIG	634	484	438	564	0.86	0.77	1.37
$\{\text{Eu}_{0.75}\text{Sm}_{0.25}\}$ IG	628	467	455	561	0.83	0.81	1.36

²⁹ J. M. Baker and F. I. B. Williams, Proc. Roy. Soc. (London) **A267**, 283 (1962).

TABLE IV. Effective magnetic fields and anisotropy parameters giving the best fit to experimental results, assuming \mathbf{n}_d to be in the (001) plane. s.p.=relative site population.

Compound	T(°K)	H_{eff} (kOe)				\bar{H}_{eff} (kOe)	μ_x	μ_y	μ_z	δ
		s.p.=2	s.p.=2	s.p.=1	s.p.=1					
Eu ³⁺ in SmIG	4.2	680	599	484	438	566	0.86	0.77	1.37	7°
Eu ³⁺ in SmIG	20	668	572	533	468	576	0.92	0.81	1.26	12°
{Eu _{0.6} Sm _{0.6} }IG	4.2	656	605	473	450	562	0.85	0.79	1.36	6°
{Eu _{0.75} Sm _{0.25} }IG	4.2	651	605	469	452	559	0.85	0.79	1.36	4°
{Eu _{0.95} Sm _{0.05} }IG	4.2	668	610	490	478	576	0.85	0.82	1.33	5°

quite good—indicating that \mathbf{n}_d , the direction of the magnetization of the Fe³⁺ ions at the d site, is approximately in the [111] direction in EuIG and in the [110] direction in SmIG and in the mixed Eu-Sm garnets. The large difference found between the values of μ_x , μ_y , and μ_z proves that the Eu-Fe exchange interaction is very anisotropic.

Better fits to the experimental spectra can be obtained by splitting the spectrum corresponding to the high multiplicity site in SmIG and in the mixed Eu-Sm garnets into two spectra of equal intensities with fields differing by about 10%, thus resulting in four subspectra with relative intensities of 2:2:1:1. The solid lines in the 4.2° and 20°K spectra in Fig. 1 and in the mixed {Eu-Sm}IG spectra in Fig. 2, are the theoretical spectra obtained assuming four sites with different fields. The values of $|\mathbf{H}_{\text{eff}}|$ which gave the best fit (the least sum of square deviations from the experimental points) in each case are summarized in Table IV. Four Eu³⁺ magnetically inequivalent sites with relative multiplicities 2:2:1:1 exist if \mathbf{n}_d is not exactly in the [110] direction of the crystal, but lies in the (001) plane and makes a small angle δ with the [110] direction. From the values of H_{eff} at the Eu nuclei in the four sites, as obtained from the best computer fits to the spectra, the values of \bar{H}_{eff} , μ_x , μ_y , μ_z , and δ were derived. These values are given in Table IV. We estimate the possible errors on the values of μ_x , μ_y , and μ_z to be ± 0.04 and the possible errors on δ to be $\pm 2^\circ$. (The values of δ given in Table IV provide the best fit to the experimental data consistent with the assumptions mentioned above.) It is seen that the anisotropy parameters obtained from the analysis assuming four sites with relative multiplicities 2:2:1:1 (Table IV) are almost identical with those obtained from the analysis assuming three sites with relative multiplicities 4:1:1 (Table III).

The emission spectrum of SmIG at 20°K is clearly different from that obtained at 4.2°K. It can be fitted by assuming that \mathbf{n}_d is in the (001) plane. The reconstructed spectrum is then composed of four subspectra corresponding to $\bar{H}_{\text{eff}}=576$ kOe and $\mu_x=0.92$, $\mu_y=0.81$ and $\mu_z=1.26$, and $\delta=12^\circ$. These anisotropy parameters are different by about 7% from those obtained at 4.2°K by assuming that \mathbf{n}_d is in the (001) plane. With the conventional assumptions made in the analysis of Mössbauer spectra, we cannot fit the 20°K spectrum by as-

suming that the magnetization is exactly in the [110] direction.

The general shape of the absorption spectra of SmIG at 85°K (Fig. 1) is similar to that of EuIG at 4.2°K (Fig. 2), indicating that the direction of \mathbf{n}_d in SmIG at 85°K is close to the [111] direction. We cannot get an exact fit to the spectrum of SmIG at 85°K by assuming that \mathbf{n}_d is exactly in the [111] direction. The theoretical spectrum expected with \mathbf{n}_d in the [111] direction is presented by the solid line in the EuIG spectrum of Fig. 2, which is quite different from the experimental spectrum of SmIG at 85°K. In order to obtain a good fit to the SmIG spectrum at 85°K, an angle of 10° between \mathbf{n}_d and the [111] direction has to be assumed (solid line in the 85°K spectrum of Fig. 1).

The recoilless absorption spectrum of {Eu_{0.95}Sm_{0.05}} IG at 20°K shows that, at this temperature, the direction of \mathbf{n}_d for this mixed garnet is close to the [111] direction.

In the theoretical spectra where canting was taken into account, it was assumed that \mathbf{n}_d is in a fixed direction. It is clear that the spectra could also be fitted by assuming a small random canting.

We have remeasured, at 4.2°K, the recoilless absorption spectrum of the 103-keV γ ray of Eu¹⁵³ emitted from a Sm¹⁵³IG source in a Eu₂O₃ absorber. The spectrum obtained is similar to that given in Ref. 16, but is much more symmetrical. The asymmetry of the spectrum obtained in Ref. 16 was due to the presence of small amounts of Sm₂O₃ impurities in the source. The Sm¹⁵³IG spectrum is consistent with the interpretation that it is composed of three subspectra corresponding to internal hyperfine fields of 630, 467, and 455 kOe with relative intensities of 4:1:1 (see Table III).

B. Recoilless Absorption Measurements of the 14.4-keV γ Ray of Fe⁵⁷

As an additional check to our conclusion that the magnetization in SmIG at low temperatures is along the [110] direction, recoilless absorption spectra of the 14.4-keV γ ray of Fe⁵⁷ in SmIG and EuIG were performed at 4.2, 20, 85, and 300°K. The spectra obtained at 85 and 4.2°K are shown in Figs. 4 and 5. It is clearly seen that, whereas the two spectra at 85°K are almost identical, there is a very significant difference between the spectra

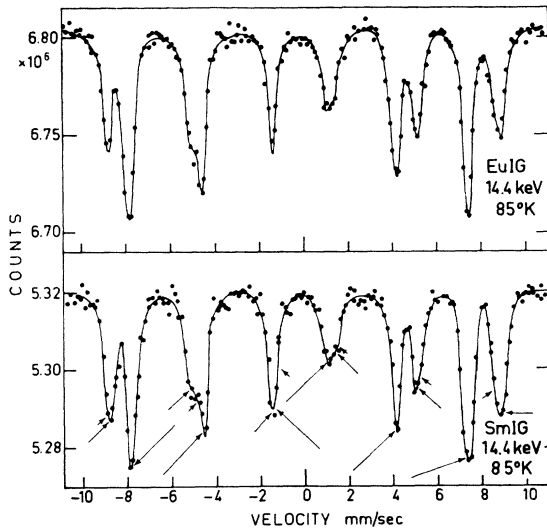


FIG. 4. Recoilless absorption spectra of the 14.4-keV γ ray, emitted from a Co^{57} source, in EuIG and SmIG absorbers at 85°K. The arrows in the SmIG spectrum indicate the calculated position of the lines, computed with the parameters given in Table VI. (The calculated positions of the lines in the EuIG spectrum are identical to those in the SmIG spectrum.) The length of each arrow is proportional to the population of the site associated with the respective line.

taken at 4.2°K. Such a difference between the two spectra is expected if the direction of \mathbf{n} at 4.2°K is close to the [111] direction in EuIG and to the [110] direction in SmIG. Because of the difference in the angles between the directions of \mathbf{H}_{eff} and the local crystalline-symmetry axes at the Fe^{3+} sites in the two garnets, the effective quadrupole-interaction parameters $\epsilon_{\text{eff}} = \frac{1}{4}eqQ \times [\frac{1}{2}(3 \cos^2\theta - 1)]$ in EuIG and SmIG will be very different (θ is the angle between \mathbf{H}_{eff} and the local symmetry axis). The symmetry axes of the d sites in the garnets are along the principal axes of the unit cell and those of the a sites are along the diagonals of the cubic unit cell. The resulting relative populations of the sub-sites and the values of $\cos\theta$ and ϵ_{eff} are summarized in Table V. (θ and θ' are the angles between the direction of the local symmetry axis and the [111] and [110] directions, respectively; $\epsilon_d = \frac{1}{4}eq_dQ$ and $\epsilon_a = \frac{1}{4}eq_aQ$, where q_d and q_a are the electric field gradients at the Fe nuclei in the d and a sites, respectively, and Q is the quadrupole moment of the 14.4-keV level of Fe^{57} .)

TABLE V. Relative population of sites and effective quadrupole interactions in Fe^{57} in the various sites in iron garnets. s.p. = relative site population.

Iron site	\mathbf{n} along [111] direction			\mathbf{n} along [110] direction		
	s.p.	$\cos\theta$	ϵ_{eff}	s.p.	$\cos\theta'$	ϵ_{eff}
Tetrahedral d'	6	$\frac{1}{3}\sqrt{3}$	0	4	$\frac{1}{2}\sqrt{2}$	$\frac{1}{4}\epsilon_d$
Tetrahedral d''				2	0	$-\frac{1}{2}\epsilon_d$
Octahedral a'	1	1	ϵ_a	2	0	$-\frac{1}{2}\epsilon_a$
Octahedral a''	3	$\frac{1}{3}$	$-\frac{1}{3}\epsilon_a$	2	$(\frac{2}{3})^{1/2}$	$\frac{1}{2}\epsilon_a$

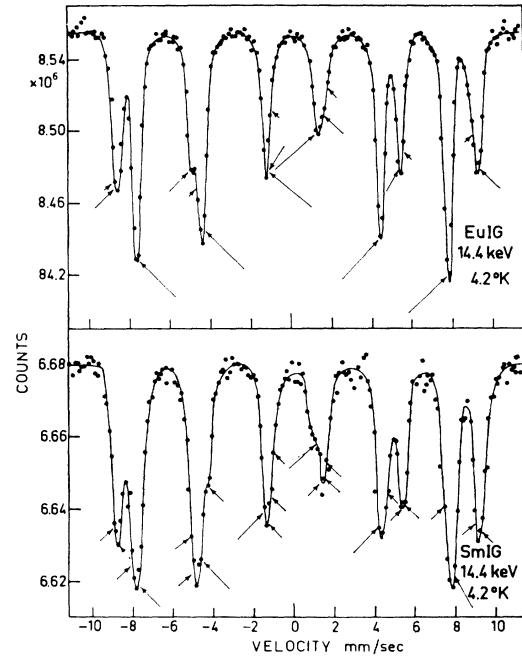


FIG. 5. Recoilless absorption spectra of the 14.4-keV γ ray, emitted from a Co^{57} source, in EuIG and SmIG absorbers at 4.2°K. The arrows indicate the calculated position of the lines, computed with the parameters given in Table VI. The length of each arrow is proportional to the population of the site associated with the respective line.

We have deduced the values of ϵ_d and ϵ_a and the isomer shift between the spectra of the Fe^{3+} ions in the a and d sites ($\Delta E_a - \Delta E_d$) from recoilless absorption measurements performed on europium iron-gallium and europium iron-scandium garnets above their Curie temperatures. These measurements are described below. The effective magnetic fields acting on the Fe nuclei in EuIG at the different sites at various temperatures are accurately known from NMR measurements.²⁰ The exact positions of the various absorption lines for the different sites were calculated for EuIG using the known hyperfine parameters. For SmIG, the same quadrupole-interaction and isomer-shift parameters as those of EuIG were used and the values of H_{eff} were chosen to fit the experimental spectra (these values are almost identical with those of EuIG). The computations were based on the tabulations of Parker,³⁰ which give the hyperfine splittings of the excited state as a function of a parameter λ , measuring the strength of the quadrupole coupling relative to the magnetic hyperfine coupling. The value of g_e/g_0 , the ratio of the g factors of the excited state and ground state in Fe^{57} , was taken as -0.571 .³¹ The parameters used in the calculations of the line positions of EuIG and SmIG at 4.2 and 85°K are summarized in Table VI. As seen from Tables V and VI, the quadrupole-splitting parameters were calculated by

³⁰ P. M. Parker, J. Chem. Phys. **24**, 1096 (1956).

³¹ G. J. Perlow, C. D. Johnson, and W. Marshall, Phys. Rev. **140**, A875 (1965).

TABLE VI. Effective magnetic fields, quadrupole interactions, and isomer shifts in the different Fe³⁺ sites, used in computing the line positions shown in Figs. 4 and 5. s.p.=relative site population.

Compound	T (°K)	Direction of magnetization	Site	s.p.	$g_0\mu_n H_{eff}$ (mm/sec)	ϵ_{eff} (mm/sec)	$\Delta E_a - \Delta E_d$ (mm/sec)
EuIG	4.2	[111]	<i>a</i>	3	6.59	0.05	0.21
			<i>a</i>	1	6.49	-0.155	
			<i>d</i>	6	5.64	0	
SmIG	4.2	[110]	<i>a</i>	2	6.59	0.078	0.21
			<i>a</i>	2	6.59	-0.078	
			<i>d</i>	4	5.72	0.12	
			<i>d</i>	2	5.52	-0.235	
SmIG, EuIG	85	[111]	<i>a</i>	3	6.52	0.05	0.21
			<i>a</i>	1	6.43	-0.155	
			<i>d</i>	6	5.58	0	

assuming that the sign of ϵ_d is positive and that of ϵ_a is negative. The spectrum of SmIG at 4.2°K can also be fitted if it is assumed that the sign of ϵ_d is negative (such an assumption was made in Ref. 35), but much better agreement is obtained with a positive value for ϵ_d . The calculated positions of the lines in the 85°K spectra, assuming \mathbf{n} to be in the [111] direction are indicated in Fig. 4. They are seen to be in very good agreement with the position of the lines in the experimental recoilless absorption spectra of the 14.4-keV γ ray in EuIG and in SmIG at 85°K. In Fig. 5, the calculated positions of the lines, assuming \mathbf{n} to be in the [111] direction in EuIG and in the [110] direction in SmIG at 4.2°K, are shown. Again the agreement between the calculated and the experimental positions is very good. These measurements strongly support our previous conclusion that the direction of \mathbf{n} is close to the [110] direction in SmIG at 4.2°K and close to the [111] direction in SmIG at 85°K and in EuIG at all temperatures measured. The recoilless absorption spectra of the 14.4-keV γ ray in the garnets are not sensitive enough to detect small deviations of the direction of magnetization from the [111] or [110] directions.

The recoilless absorption spectrum of the 14.4-keV γ ray in SmIG at 20°K is very similar to the one obtained at 4.2°K, indicating that at this temperature \mathbf{n}

in SmIG is still close to the [110] direction. The recoilless absorption spectra obtained at 300°K for SmIG and EuIG absorbers were almost identical. (The fields in SmIG are 3% larger than in EuIG.) These results are in disagreement with the conclusions of Van Loef,³² which state that the direction of easy magnetization in SmIG is along the [110] direction even at 295°K.

C. Quadrupole Interactions in Fe⁵⁷ in *a* and *d* Sites of Garnets

The values of ϵ_d , ϵ_a , and $\Delta E_a - \Delta E_d$ were deduced from recoilless absorption measurements of the 14.4-keV γ ray in europium iron-gallium and europium iron-scandium garnets. The measurements were performed above the respective Curie temperatures of the compounds. The results are summarized in Table VII. Since the field gradients acting on the Fe⁵⁷ nuclei in the garnets are mainly produced by neighboring ions, they are not appreciably affected by the presence of the exchange field and are almost temperature-independent.

The recoilless absorption spectra of the 14.4-keV γ ray emitted from a Co⁵⁷ (in Pt) source in Eu₃Sc_{1.0}Fe_{4.0}O₁₂ and Eu₃Ga_{1.6}Fe_{3.4}O₁₄ absorbers, at 315°K, are shown in Figs. 6 and 7. The solid lines in the figures represent the theoretical spectra giving the best fit to the experimental

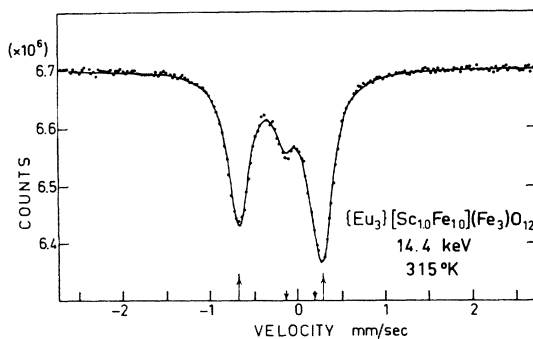


FIG. 6. Recoilless absorption spectrum of the 14.4-keV γ ray, emitted from a Co⁵⁷ source, in a Eu₃Sc_{1.0}Fe_{4.0}O₁₂ absorber at 315°K. The solid line is the theoretical spectrum computed with the parameters given in Table VII. \uparrow indicates the position of a line associated with the *d* site, and \downarrow indicates the position of a line associated with the *a* site.

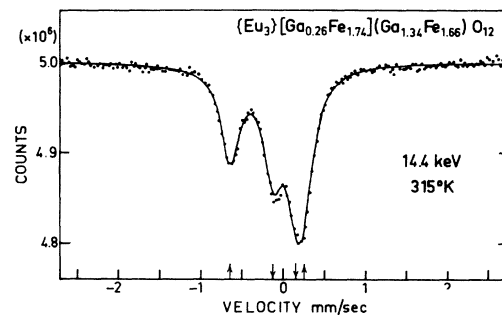


FIG. 7. Recoilless absorption spectrum of the 14.4-keV γ ray, emitted from a Co⁵⁷ source, in a Eu₃Ga_{1.6}Fe_{3.4}O₁₄ absorber at 315°K. The solid line is the theoretical spectrum computed with the parameters given in Table VII. \uparrow indicates the position of a line associated with the *d* site, and \downarrow indicates the position of a line associated with the *a* site.

³² J. J. van Loef, J. Appl. Phys. **39**, 1258 (1968).

TABLE VII. Quadrupole interactions and isomer shifts in Fe⁵⁷ in the two Fe³⁺ sites, as measured in substituted RIGs above their Curie temperatures.

Garnet	Curie temp. (°K)	Temperature of measurement (°K)	$ \epsilon_d $ (mm/sec)	$ \epsilon_a $ (mm/sec)	$\Delta E_a - \Delta E_d$ (mm/sec)	Ref.
{Eu ₃ }[Ga _{0.26} Fe _{1.74}] (Ga _{1.34} Fe _{1.66})O ₁₂	298 ^a	315	0.45 ± 0.02	0.17 ± 0.015	0.21 ± 0.02	this work
{Eu ₃ }[Sc _{1.0} Fe _{1.0}] (Fe ₂)O ₁₂	300 ^b	315	0.485 ± 0.015	0.16 ± 0.02	0.22 ± 0.02	this work
{Eu ₃ }[Sc _{1.5} Fe _{0.5}] (Fe ₃)O ₁₂	30 ^b	290	0.49 ± 0.015	0.15 ± 0.02	0.21 ± 0.02	this work
YIG			0.465 ± 0.010	0.235 ± 0.010	0.23 ± 0.07	36
{Y _{3-x} Ca _x }Fe _{0.5-x} Sn _x O ₁₂ (av.)			0.50 ± 0.03	0.24 ± 0.02	0.26 ± 0.03	36
RIG (av.)			0.46 ± 0.03	0.23 ± 0.03	0.22 ± 0.05	35

^a Reference 34.^b Reference 18. (The Curie temperatures given here are those of Sc substituted for GdIGs.)

spectra from which the parameters given in Table VII were deduced. The third spectrum was similar in shape to the two shown in the figure and was analyzed in the same way. As was known from previous measurements,¹⁸ and verified in the present work, Sc ions substitute for the Fe ions in the *a* site only, whereas Ga ions replace preferentially the Fe³⁺ ions in the *d* sites, but occupy the *a* sites, as well.^{7,26,33,34} The numbers of Ga and Sc ions in each site were also derived from the best theoretical fit to the experimental spectra, assuming equal recoil-free fractions at the *a* and *d* sites. The numbers found for the europium iron-gallium garnet agreed very well with those given in Ref. 7. (The same Eu₃Ga_{1.6}Fe_{3.4}O₁₂ sample was used in the present work and in the work described in Ref. 7.) For comparison, Table VII also includes quadrupole-interaction and isomer-shift parameters obtained in previous works for pure RIGs^{35,36} and for yttrium iron-tin garnets.³⁶ The results obtained in the present work are in good agreement with the previous results for the *d* sites, but differ for the *a* sites. The averages of the parameters obtained in the present work were used in the calculations of the theoretical recoilless absorption spectra of the 14.4-keV γ ray in pure EuIG and SmIG at various temperatures, as described in the previous paragraph.

CONCLUSIONS

The experimental results reported in the previous sections lead to the following conclusions:

(a) The Eu-Fe exchange interaction in the garnets is anisotropic. The anisotropy parameters are $\mu_x = 0.85 \pm 0.08$, $\mu_y = 0.78 \pm 0.08$, and $\mu_z = 1.37 \pm 0.14$.

(b) The anisotropic properties of the Eu³⁺ ion in the garnets are mainly produced by the anisotropy in the

Eu-Fe exchange interaction and not by the crystalline-field interactions.

(c) The values of G_2^0 and G_2^2 derived from the experimental values of μ_x , μ_y , and μ_z , using Eq. (14) are $G_2^0 = 0.021 \pm 0.002$ and $G_2^2 = -0.0055 \pm 0.0005$ for A_2^2 positive ($G_2^2 = +0.012$ for A_2^2 negative). These values may be compared with those obtained by Wickersheim and White³⁷ for YbIG: $G_2^0 = -0.03$ and $G_2^2 = 0.07$. It is seen that the values for YbIG are very different from the values derived here for EuIG. The value of G_2^2/G_2^0 is about 2 for Yb, whereas it is ~ 0.25 (A_2^2 positive) for Eu. Since it is reasonable to believe that the parameters G_2^0 and G_2^2 should be approximately the same for all of the rare-earth ions, the difference obtained here tends to show that there is no justification for taking only the first three (out of the ten) terms in the expansion of $J(L_x, L_x)$ in Eq. (2) into account. The contributions of the higher terms to the RE-Fe exchange interactions in the garnets cannot be neglected.

(d) The direction of the tetrahedral iron sublattice magnetization (\mathbf{n}_d) in SmIG at 4.2 and 20°K and in mixed {Eu-Sm}IG at 4.2°K is close to the [110] direction. The direction in SmIG above 85°K is close to the [111] direction.

(e) With the conventional assumptions made in the analysis of Mössbauer spectra, we could not fit the emission spectrum of SmIG at 20°K by assuming that \mathbf{n}_d is exactly in the [110] direction nor the emission spectrum at 85°K by assuming that \mathbf{n}_d is exactly in the [111] direction. The agreement between the theoretical and the experimental spectra of SmIG and mixed Eu-Sm garnets at 4.2°K is improved if it is assumed that \mathbf{n}_d is canted relative to the [110] direction.

ACKNOWLEDGMENT

We are grateful to P. M. Levy for making several important suggestions concerning the theory of anisotropic exchange.

³⁷ These are the values recalculated by R. L. White (private communication) from the experimental data given in Ref. 2.

³³ M. A. Gilleo and S. Geller, Phys. Rev. **110**, 73 (1958).

³⁴ B. Luthi and T. Henningsen, in *Proceedings of the International Conference on Magnetism, Nottingham, 1964* (The Institute of Physics and the Physical Society, London, 1965), p. 668.

³⁵ W. J. Nicholson and B. Burns, Phys. Rev. **133**, A156 (1964).

³⁶ I. S. Lyubutin, E. F. Makarov, and V. A. Povitsky, Zh. Eksperim. i Teor. Fiz. **53**, 65 (1967) [English transl.: Soviet Phys.—JETP **26**, 44 (1967)].